

Surface Modification of Silk Fibroin Nanofibrous Mat with Dextran for Wound Dressing

Moo Kon Kim¹, Hyo Won Kwak¹, Hyung Hwan Kim¹, Tae Rin Kwon², So Young Kim², Beom Joon Kim³, Young Hwan Park¹, and Ki Hoon Lee^{1,4,5*}

¹Department of Biosystems & Biomaterials Science and Engineering, Seoul National University, Seoul 151-921, Korea

²Major in Biomedical Science, Department of Medicine, Graduate school, Chung-Ang University, Seoul 156-755, Korea

³Department of Dermatology, Chung-Ang University College of Medicine, Seoul 156-755, Korea

⁴Center for Food and Bioconvergence, Seoul National University, Seoul 151-921, Korea

⁵Research Institute for Agriculture and Life Sciences, Seoul National University, Seoul 151-921, Korea

(Received October 7, 2013; Revised December 2, 2013; Accepted December 10, 2013)

Abstract: In this study, we examined the effects of a dextran-modified silk fibroin nanofibrous mat (D-SFNM) on wound healing. To increase the hydrophilicity of silk fibroin (SF), the SF nanofibrous mat (SFNM) was modified with oxidized dextran. The D-SFNM absorbed water faster than the SFNM, and the swelling ratio was increased by approximately 80 % compared with the SFNM. An *in vitro* cell (NIH3T3) test revealed that fewer cells attached to the D-SFNM than the SFNM, but the proliferation of cells was not significantly affected by the presence of dextran. An *in vivo* wound healing test with mice indicated that the D-SFNM resulted in a good wound recovery effect similar to a commercial wound dressing material. The increased hydrophilicity of the D-SFNM might balance the moist environment at the wound site, which improves the wound healing compared with the SFNM.

Keywords: Silk fibroin, Dextran, Wound healing, Wound dressing, Surface modification

Introduction

The wound healing process includes a series of independent and overlapping stages: hemostasis, inflammation, migration, proliferation and maturation [1]. In each stage, multiple levels of cellular and molecular events should be activated properly to successfully heal a wound. Since the 1960s-1970s, the moisture balance at the wound bed has been identified as one of the essential requirements of successful wound healing [2-4]. Exudates at the wound bed maintain a moist environment and promote cellular growth or collagen proliferation by promoting the action of growth factors (platelet-derived growth factor, transforming growth factor, epidermal growth factor, etc.), cytokines and chemokines [4]. However, some types of wounds, such as venous ulcers or burn injuries, produce more exudate, and these excessive exudates can induce problems, such as the formation of necrotic tissue by bacterial growth, which leads to infection or pain [1-3]. Therefore, the moisture at the wound bed should be balanced.

Silk fibroin (SF), which is produced by silkworms, is biocompatible and biodegradable and has a low cytotoxicity [5-7]. Therefore, this natural polymer is considered a superior material in the biomedical field and used in various different forms, such as fibers [8], nanomats [9], sponges [10], films [11], hydrogels [12] and micro- or nanoparticles [13]. Specifically, it can promote the proliferation of human keratinocytes or fibroblasts. SF has been identified as a good candidate in wound dressing. SF films were reportedly

effective for epidermal recovery from full-thickness skin wounds [14] and cutaneous burn wounds [15]. Min *et al.* [16] compared the cellular response of human keratinocytes to the SF microfiber, film and nanofiber material. They speculated that the SF nanofiber is a more preferable wound dressing material compared with the others. Furthermore, several parameters that affect the wound healing process, such as absorption, water vapor transmission, oxygen permeability and enzyme biodegradation, could be controlled by changing the diameter and porosity of the SF nanofiber mat [17]. Sometimes, growth factors or antimicrobial agents have been loaded into the SF nanofiber to increase the biofunctionality for wound healing [18,19]. Although these past results suggest that SF is suitable for wound dressing, SF alone cannot satisfy all the requirements of modern wound dressing materials. For example, SF has a high content of hydrophobic amino acids, such as glycine and alanine, and could be made insoluble by the formation of β -sheet conformations or a crystalline structure. Therefore, the water absorption or swelling of SF is poor. Furthermore, it is inadequate in terms of maintaining the moist environment at the wound site. If the hydrophilicity of SF can be enhanced, the SF can provide an improved moist environment at the wound site. To improve the inherent properties of SF, several hydrophilic polymers, such as elastin [20], chitosan [21], alginate [22], gelatin [23] and sericin [24], were blended with SF. This incorporation improved the wound recovery compared with the neat SF.

Conversely, naturally derived polysaccharides are also ideal materials in biomedical fields, such as tissue engineering or drug delivery, due to their biocompatibility and

*Corresponding author: prolee@snu.ac.kr

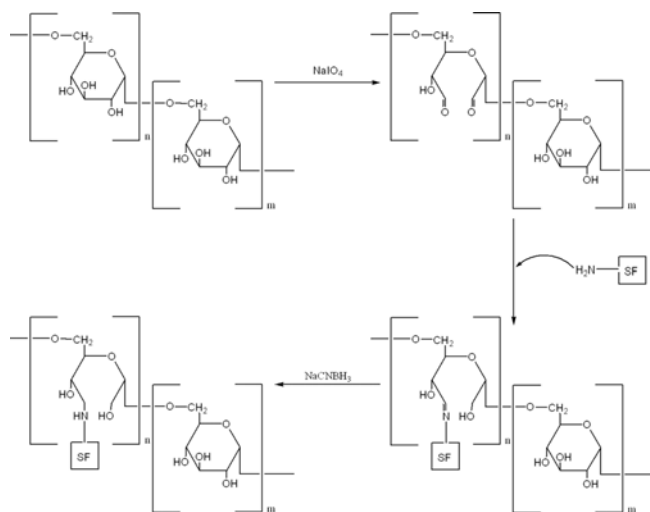


Figure 1. Introduction of dialdehyde groups to dextran by oxidation and crosslinking to SFNM by Schiff base formation.

biodegradability [25–28]. In essence, they consist of common monosaccharide monomers. However, they have diverse properties that depend on the monomer type and O-link and are applied to different areas. Dextran is a type of polysaccharide that has α -1, 6 glycosidic links. It is biocompatible and easily degraded by dextranases in the human body and stimulates the activity of cells that participate in wound recovery. Therefore, dextran has also been applied as a wound dressing alone or with other polymers [29–33]. Because dextran has many hydroxyl groups, it has a good water binding capacity. The incorporation of dextran can enhance the hydrophilicity of the host material.

To endow SF with hydrophilicity, we conjugated dextran onto the SF nanofibrous mat (SFNM). Dextran was oxidized by sodium periodate, and dialdehyde groups were introduced at the C2–C3 links. Aldehydes of oxidized dextran were conjugated with amine groups via the Schiff base formation followed by reductive amination (Figure 1). After crosslinking the oxidized dextran to SFNM, we evaluated the water binding capacity of dextran-crosslinked SF nanomats (D-SFNM) and compared their clinically effect on skin regeneration with commercially used dressing materials via an *in vivo* test.

Experimental

Materials

Dextran (from *Leuconostoc mesenteroides*, MW 64,000–76,000), sodium periodate, sodium cyanoborohydride, pH 8.0 Trizma hydrochloride buffer solution, 3-(4,5-dimethylthiazol-2-yl)-2,5-diphenyl tetrazolium bromide (MTT) and other reagents were purchased from Sigma Aldrich (USA). A dialysis membrane (MWCO 6–8,000) was purchased from Spectra/Por® (USA). *Bombyx mori* cocoons were purchased

from Heungjin (Korea). Dimethyl sulfoxide (DMSO) was purchased from Amresco (USA), and methanol was purchased from Samchun (Korea). Phosphate buffered saline (Dulbecco modified phosphate buffer saline, DPBS), Dulbecco modified Eagle's minimal essential medium (DMEM) and penicillin streptomycin solution were purchased from Corning (USA). Fetal bovine serum (FBS) was purchased from Omega Scientific Inc. (USA).

Preparation of SF Nanofibrous Mat

B. mori cocoons were degummed twice with 0.2 % (w/v) sodium carbonate and 0.3 % (w/v) Marseille soup solution at 100 °C for 30 min and rinsed with distilled water to remove silk sericin. The extracted SF was dissolved in a calcium chloride/ethanol/distilled water (1:2:8, molar ratio) solution at 80 °C for 5 min and dialyzed for three days against distilled water. The dialyzed solution was lyophilized to obtain the SF powder. The SF powder was dissolved in formic acid at 13 % (w/v) for 6 h and electrospun. The applied voltage was 13 kV and the flow rate was 0.3 ml/hr. The SFNM was soaked in methanol for 2 h and dried at room temperature.

Surface Modification of SF Nanofibrous Mat with Dextran

Dextran (4.28 g) was dissolved in 500 ml of a 0.03 M sodium periodate solution (molar ratio of dextran to sodium periodate was approximately 1:1). The mixture was maintained overnight at room temperature in the dark and dialyzed for two days against distilled water. After lyophilizing, the oxidized dextran was obtained. The oxidized dextran was dissolved at 1.5 % (w/v) in 100 ml of 0.1 M sodium phosphate buffer solution containing 0.15 M sodium chloride. SFNM (0.15 g) was then soaked in the oxidized dextran solution and 20 ml of 1 M sodium cyanoborohydride was added. The reaction continued overnight. After the reaction, 20 ml of pH 8.0 Trizma hydrochloride was added to the solution to block any excess unreacted aldehyde groups. After 2 h, the D-SFNM was washed with distilled water and dried. The surface images of SFNM and D-SFNM were obtained with a field emission scanning electron microscope (FE-SEM) (JSM-7600F, JEOL, JAPAN), and the elemental composition of the surface of the SFNM and D-SFNM were analyzed with an energy dispersive X-ray spectrometer (EDS) (SUPRA 55VP, Carl Zeiss, Germany).

Wettability Test

We determined the wettability of SFNM and D-SFNM with a contact angle test and swelling test. The contact angle test was performed on a drop shape analyzer (DSA100, KRÜSS, Germany) with the sessile drop method by using a 10 μ l water droplet. The swelling ratios of SFNM and D-SFNM were determined as follows: The samples were cut into circles (2.5 cm in diameter) and incubated in 10 mM PBS (pH 7.4) at 37 °C. After 2 h, the water on the surface of

samples was removed with filter paper. The swelling ratios of samples were calculated by following formula:

$$\text{Swelling ratio (\%)} = \frac{W_s - W_d}{W_d} \times 100$$

where W_s is the swollen weight and W_d is the weight before swelling.

Cytotoxicity Test

The cytotoxicity was determined with a MTT test. Before the test, the samples were sterilized with 70 % EtOH for 3 h and washed three times with DPBS. Fibroblasts (NIH3T3) were seeded at 1.5×10^5 cells per sample in DMEM containing 10 % FBS and 1 % penicillin-streptomycin solution into 96-well plates and incubated in 5 % CO₂ and 95 % air in an incubator at 37 °C. After the incubation period, 200 μ l of 0.5 mg/ml MTT was added to each sample, and the mixture was incubated for 4 h at 37 °C in 5 % CO₂ and 95 % air in an incubator. After removing the MTT solution, the samples were washed two times with DPBS and 200 μ l of DMSO was added. Supernatants were removed and formazan crystals resulting from mitochondrial enzymatic activity on MTT substrate were solubilized with DMSO. After 30 minutes, the UV absorbance at 490 nm was read with a microplate reader (Synergy H1, Biotek, USA).

Evaluation of Healing Effect on Wound of Dressing Materials

Animal Test

Six-week-old male nude (*nu/nu*) BALB/c mice (Charles River Laboratories, Wilmington, MA) of 18-20 g body weight were used for all experiments. The experimental subjects were six-week-old male nude (*nu/nu*) BALB/c mice who were stabilized for seven days before wound induction. The circular wounds (1.5 cm diameter) were induced with an erbium laser (CB 2.94, Hoya ConBio, USA) at 8 Hz and 0.6 J/cm² (Figure 2). Each dressing material was sterilized by 70 % EtOH and transplanted into the wound. Each wound area was closed with SFNM, D-SFNM or Medifoam[®] as the positive control. The size of each wound from individual mouse were measured and tissue samples were taken for biopsy at 4, 7, 11 and 15 days after the wound induction. Anesthesia was performed by intra peritoneal injection with a mixture of anesthesia with Zoletil (30 mg/kg) and Rompun (10 mg/kg) mixture. The percentage of wound area was calculated following formula:

$$\% \text{ of wound healed} = \frac{S_w - S_H}{S_w} \times 100$$

where S_w is the size of the wound area before dressing and S_H is the size of the wound area after healing. The animal test was approved by the Institutional Animal Care and Use Committee, Chung-Ang University (IRB 12-0033) and carried out under their guidelines.

Histological Examination

The skin tissues taken from each mouse were fixed with a 10 % natural buffered formalin solution for 24 h and embedded in paraffin. For morphological observation, the sections were then prepared and stained with Hematoxylin & Eosin (H&E). For collagen staining and elastic tissue staining, the paraffin-fixed samples were deparaffinized with xylene and washed with distilled water. For collagen staining, the samples were primarily fixed in formalin and secondarily fixed in Bouin solution at 56 °C for 1 h. Subsequently, the picric acid on the colored samples were removed and stained with Weigert's iron hematoxylin for 10 min. After washing with distilled water, the samples were stained with a 0.9 % Biebrich scarlet-acid fuchsin solution for 15 min and stained again with a phosphomolybdic phosphotungstic acid solution (phosphomolybdic 2.5 g and phosphotungstic acid 2.5 g in distilled water 100 ml) for 15 min. Finally, the samples were stained with a 2 % light green solution for 5 min and washed a 1 % acetic acid solution. Each stained section was dehydrated before observation with the microscope. The elastic tissue was stained by Verhoeff Van Gieson (EVG) staining. The washed sections were stained with Verhoeff solution for 30 min and washed with distilled water. Under the microscope, the samples were decolorized with a 2 % ferric chloride solution until the color of elastic tissues turned to black. After washing with distilled water, the colored iodine was removed with a 5 % sodium thiosulfate solution. Lastly, the negative staining was performed in a Van Gieson solution for 3 min. The images were captured by the Olysia Soft Imaging System (Olympus Optical Co., Tokyo, Japan).

Results and Discussion

Surface Modification of SF Nanofibrous Mat Using Dextran

The surface of SFNM can be modified by many different methods because SF has many functional groups, such as amino, hydroxyl and carboxyl groups. Conversely, dextran has hydroxyl groups, which are available for chemical reactions. However, the reactivity of hydroxyl groups is not as high as that of amino and carboxyl groups and often requires harsher reaction conditions that can damage the SFNM. The oxidation of hydroxyl groups at C2 and C3 of polysaccharides is a well-known reaction, and it converts the hydroxyl groups into aldehydes and finally into carboxyl groups. Aldehydes are very active functional groups that easily react with amino groups to form Schiff bases. This strategy has previously been used to covalently bond several molecules to polysaccharides [34-36]. We adopted the same strategy to modify the surface of SFNM. The advantage of this method is that it does not require an additional crosslinking agent, which could be harmful to the final intended use if not successfully removed. Figure 1 shows the chemical reaction scheme used in this study to modify SFNM using dextran. Sodium periodate was used to oxidize the hydroxyl groups

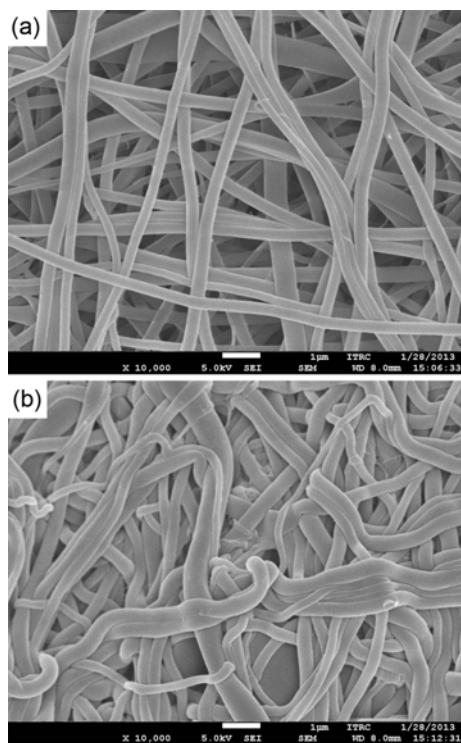


Figure 2. FE-SEM images of SFNM (a) and D-SFNM (b).

Table 1. Atomic concentrations (%) of SFNM and D-SFNM surfaces by elemental analysis with EDS

	C (%)	N (%)	C/N
SFNM	55.68±1.09	26.20±0.85	2.13±0.08
D-SFNM	61.55±1.13	24.37±0.57	2.53±0.11

at C2 and C3 of dextran into aldehyde groups [30]. The newly formed aldehyde groups could covalently bond with the amino groups of SF by forming a Schiff base. The Schiff base is not stable for a long-term use. Therefore, we reduced it by using sodium cyanoborohydride. Figure 2 shows the

morphology of the SFNM before and after modification with dextran. The initial diameters of the SF nanofiber were 335 ± 47 nm. After the surface modification with dextran, the diameters of the SF nanofibers slightly increased (429 ± 52 nm). However, this increase in diameter was due to the swelling of the SF nanofiber during the modification process rather than due to the attachment of dextran. Similar swelling effects have also been previously observed [37]. The modification with dextran was verified by EDS. Table 1 shows the results of the elemental analysis of the SFNM and D-SFNM surfaces. The D-SFNM had a higher C/N ratio than the SFNM. Because dextran does not possess nitrogen, the increase in the C/N ratio in the D-SFNM indicates that dextran was successfully coated onto the SFNM.

Wettability Test

We expected that the surface characteristics of the SFNM would differ as a result of the dextran surface modification compared with the non-modified SFNM. Initially, we attempted to determine the contact angle of a water droplet on the SFNM. However, the water droplet was absorbed too fast into the D-SFNM, making it impossible to measure the contact angle. Figure 3 shows the change in the water droplet's shape during 60 s of observation. While the water droplet on the non-modified SFNM was stable, the water droplet on the D-SFNM spread quickly and finally absorbed into the SFNM. This result shows that the surface of the SFNM was successfully modified with dextran, and the wettability of SFNM was significantly enhanced. To efficiently absorb the exudate from wounds, the dressing material must be capable of absorbing large amounts of exudate. Therefore, we determined the swelling ratio of D-SFNM (Figure 4). Compared with the SFNM, the swelling ratio of the D-SFNM was enhanced by approximately 80 %, which indicates that D-SFNM could absorb almost twice the exudate as the non-modified material. These results show that the D-SFNM wound dressing can effectively absorb exudates and provide a suitable moisture environment to the wound area.

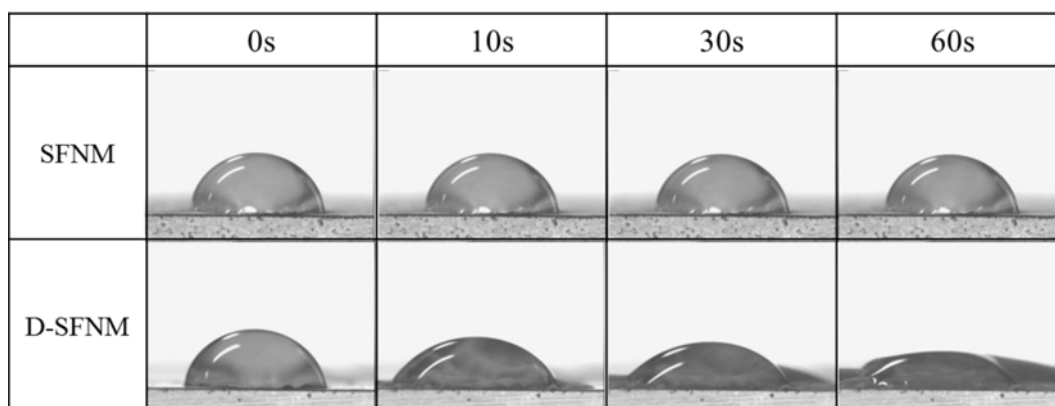


Figure 3. The wettability of SFNM and D-SFNM by contact angle. Contact angle test was performed by dropping a $10 \mu\text{l}$ water droplet on the surface of samples.

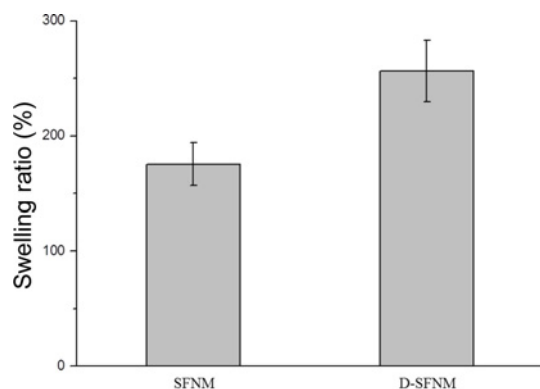


Figure 4. The wettability of SFNM and D-SFNM by swelling ratio. The swelling ratio was calculated after soaking in 10 mM pH 7.4 PBS at 37°C for 2 h (N=3).

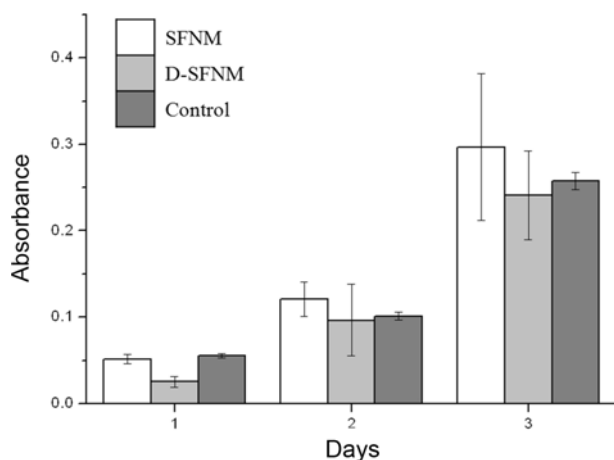


Figure 5. Cytotoxicity test of SFNM and D-SFNM. Control is the tissue culture plate (N=3).

Cytotoxicity Test

To investigate the cell viability of each sample, the cell proliferation was measured by a MTT assay. Figure 5 shows that the cell viability was lower on D-SFNM than the control and SFNM. The low cell attachment and proliferation on the D-SFNM might be due to the repelling effect of dextran or the coverage of the SFNM surface by dextran. Dextran has been reported as an alternative to poly(ethylene glycol), which inhibits the nonspecific absorption of large molecules [38]. Therefore, the cell attachment onto D-SFNM could be hindered by the presence of dextran. In addition, SF nanofibers have shown excellent cell attachment and proliferation [16]. The surface modification of SFNM with dextran could reduce the area of SF that was directly exposed to the cells. The MTT results on day 1 show that only half the number of cells on the D-SFNM survived compared with the SFNM. Gotoh *et al.* [39] observed a reduced cell attachment when PEG was conjugated with SF, and similarly, Ouchi *et al.* [40] reported that dextran-grafted polylactide films exhibited low cell attachment compared with neat polylactide. Both results agree with our results. However, when the cultivation continued, the differences between the D-SFNM and SFNM were no longer significant. Thus, cell attachment was hindered by the presence of dextran, while the proliferation of cells was not affected. This result indicates that D-SFNM had little effect on cell viability.

Wound Healing Evaluation

We observed the area of the wound site at 4, 7, 11 and 15 days after the wound induction (Figure 6 and 7). After seven days, the wound areas dressed with SFNM-transplanted mice showed the best wound closure effect compared with the other dressing materials. D-SFNM transplanted mice exhibited wound closure effects similar to those of Medifoam®

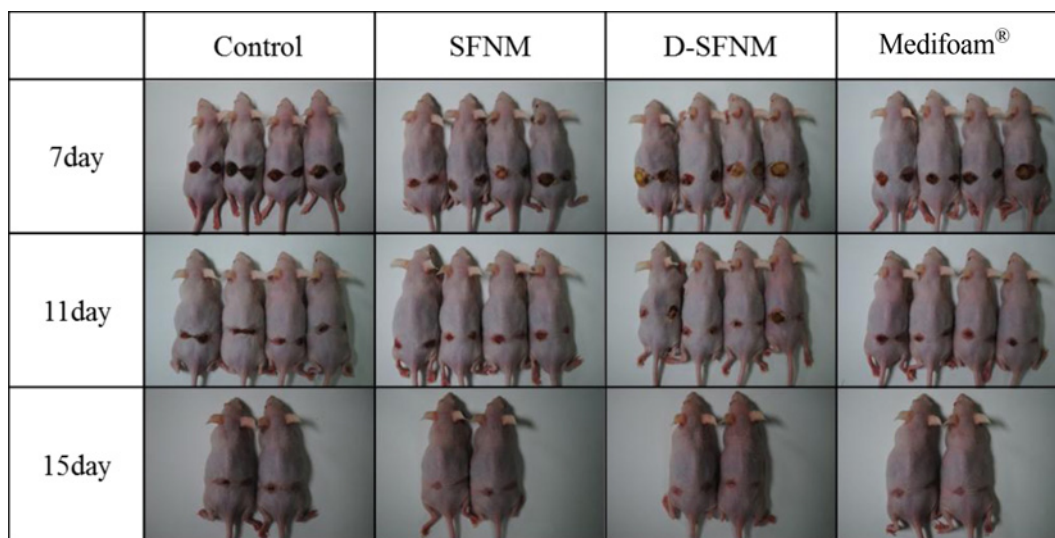


Figure 6. Optical images of wound closure of mice by days of wounding. Image analysis of wound sites was performed by image analysis device, ‘3D LifeViz (QuantifiCare, Sophia Antipolis, France)’. Time of image capture was set from 7 day, 11 day and lastly, 15 days.

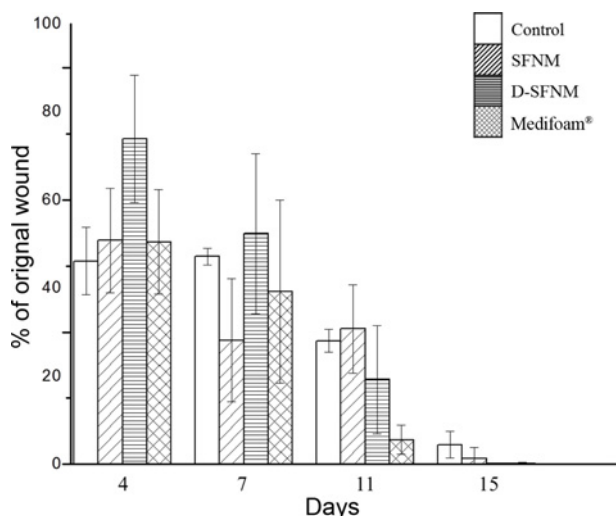


Figure 7. Percentage of wound area by calculation using photographs of the wounds by days (N=4 for 4, 7, 11 days and N=2 for 15 days except the control).

transplanted mice during this period. However, the wound area dressed with D-SFNM transplanted mice was similar to that of SFNM transplanted mice after 11 days. At the end of the study period (day 15), two of four mice showed full closure of the wound site in the SFNM, D-SFNM and

Medifoam[®] groups. D-SFNM showed the best wound closure effect, which was similar to that of Medifoam[®]. At the early stage of wound healing, SFNM may have been more favorable to the wound healing processes due to its cytotropic properties. In the case of D-SFNM, the wound healing process was faster at the last stage of wound healing. The exudate at the wound site is important because it can prevent desiccation and cell death. It also enhances epithelization and reduces hyperkeratosis. However, an excess of exudate will inhibit the proliferation and activity of cells and degrade the extracellular matrix because of tissue-degrading enzymes in the exudate, which results in delayed wound healing [1]. As shown in Figure 3 and Figure 4, D-SFNM can absorb water faster and in greater quantities compared with SFNM. As such, D-SFNM can maintain the moisture at the wound site at appropriate levels. Conversely, SFNM showed poor water absorption. Thus, it could not properly remove the exudate. The incorporation of hydrophilic polymer into SF reportedly enhanced the wound healing process. Vasconcelos *et al.* [20] prepared a wound dressing by blending and crosslinking SF and elastin. They found that wound healing was enhanced when more elastin was blended and speculated that this effect could be attributed to the improved swelling properties. Similar effects have also been reported when SF was blended with hydrophilic alginate [22]. To evaluate the reconstruction of the epidermis layer and infiltration of inflammatory cells

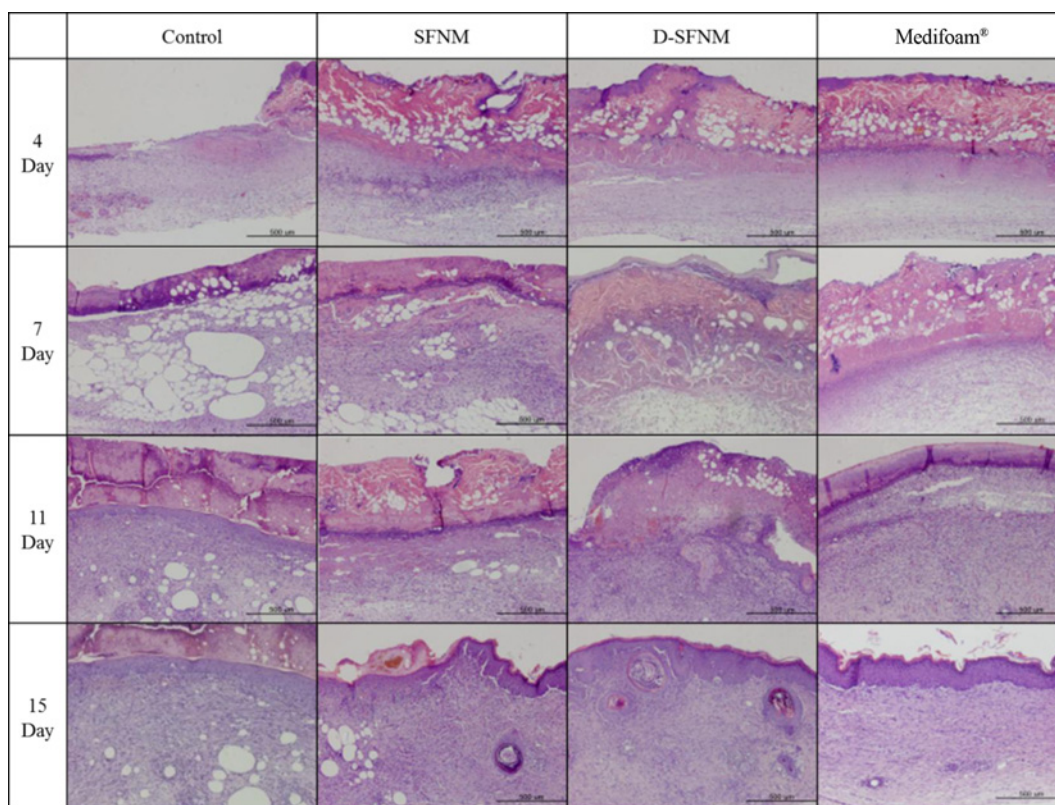


Figure 8. Histologic evaluation of skin tissue by hematoxylin and eosin staining.

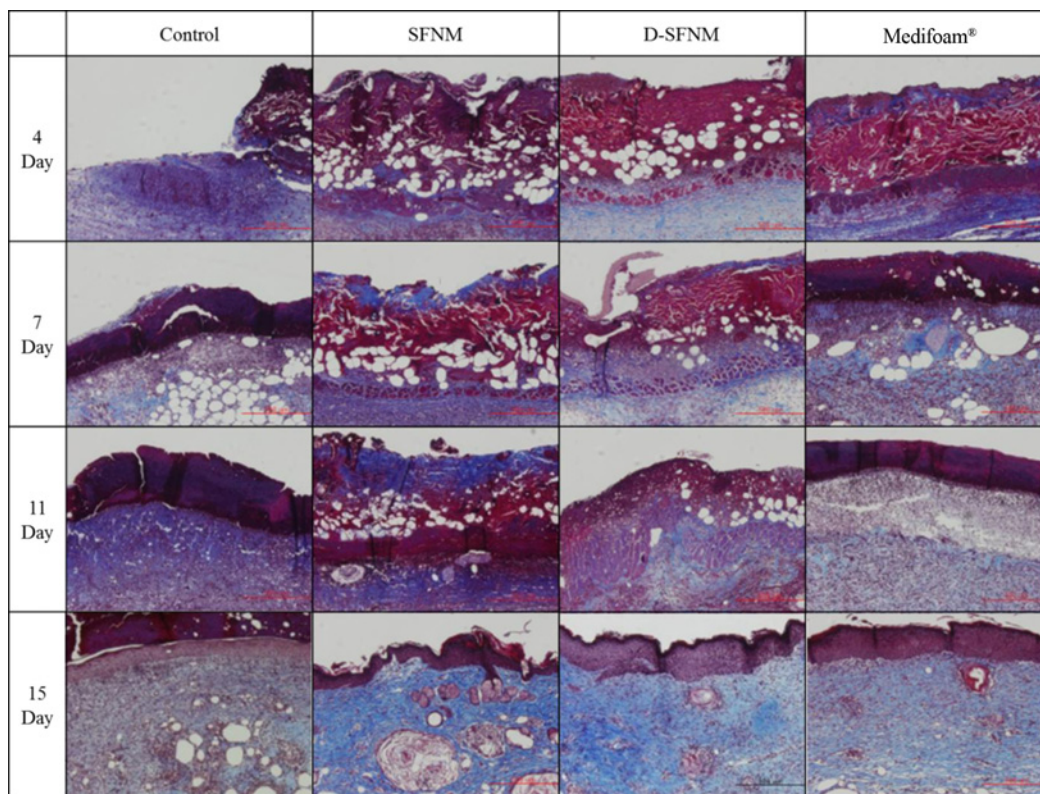


Figure 9. Observation of collagen regeneration by Masson's trichrome staining.

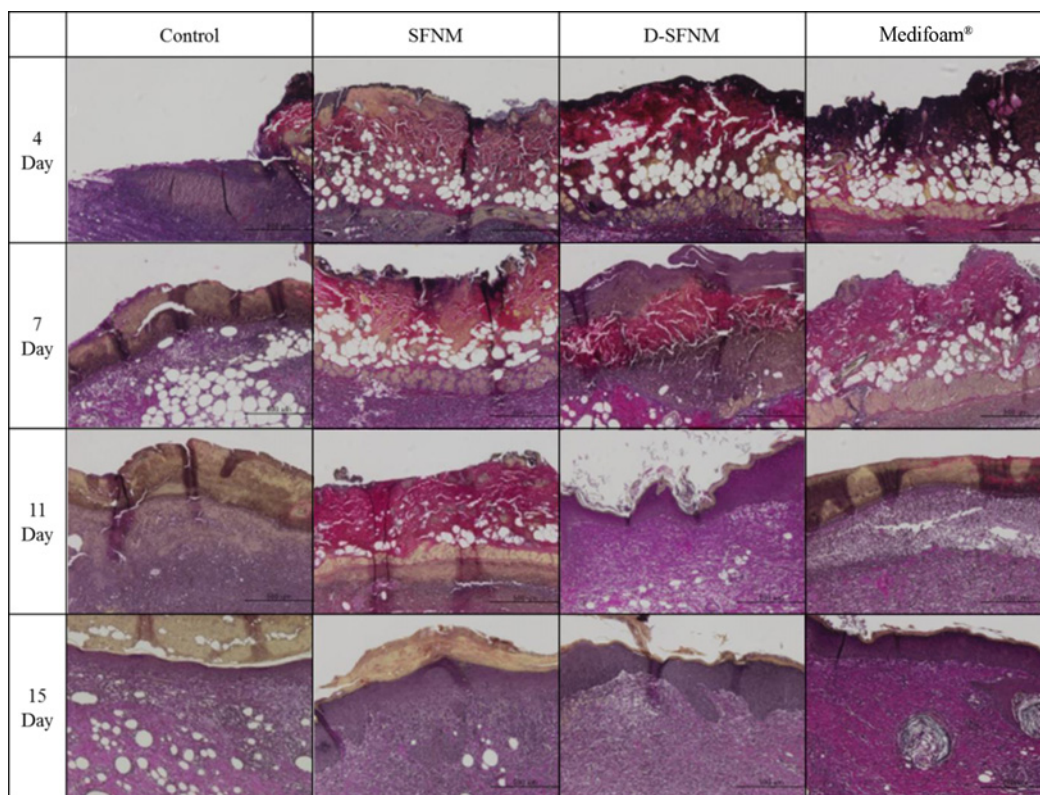


Figure 10. Observation of elastic tissue recovery by elastic Verhoeff's van Gieson staining (EVG).

into skin tissue, the tissue was stained with H&E (Figure 8). After four days, every group showed exudate and layers of inflammatory cells, such as multinuclear cells or lymphocytes on the surface layer of the wound area. However, the D-SFNM and Medifoam[®] groups showed a uniform regeneration and regular arrangement of the epithelium after day 7. Approximately 24 h after the induction of the wound, fibroblasts moved to the wound site and began to form collagen fibers. These collagen fibers formed collagen deposits or a collagenous matrix. Furthermore, a type of scar tissue and fibromas could also be induced in these processes [1]. Therefore, morphological observations of collagen fibers are significant. Figure 9 shows that collagen formation (blue) was initiated in the D-SFNM and Medifoam[®] groups after four days. After 15 days, collagen fibers filled the wound site more successfully in the D-SFNM and Medifoam[®] groups than in the control and SFNM groups. In addition, the morphology of the elastic tissue recovery was evaluated by Verhoeff's van Gieson staining (Figure 10). Elastic fibers (dark red or dark brown), which endow the skin with elasticity, were formed under the layer of the wound site at day 11 in the D-SFNM and Medifoam[®] groups. After 15 days, the D-SFNM group showed recovered elastic tissues that were more regular than those in the other groups.

Conclusion

In this study, the SFNM was modified with dextran, and its effect on wound healing was evaluated. The results show that D-SFNM is more efficient than SFNM in wound healing. The moisture balance is important during the wound healing process. The dressing material should maintain an appropriate level of exudate. The current results indicate that the enhanced water absorption of D-SFNM allows it to absorb the exudate faster, and the higher swelling ratio of D-SFNM maintains the moist environment. This result is preliminary and shows that enhancing the hydrophilicity of SF can improve the wound healing process. A more detailed study is needed in the future that optimizes the hydrophilicity of SF by changing the degree of surface modification.

Acknowledgement

This work was supported by the Seoul R&BD Program (No. JP100079C0209722) and the Marine Biomaterials Research Center grant from Marine Biotechnology Program funded by the Ministry of Oceans and Fisheries, Korea.

References

1. J. S. Boateng, K. H. Matthews, H. N. E. Stevens, and G. M. Eccleston, *J. Pharm. Sci.*, **97**, 2892 (2008).
2. D. W. Brett, *J. Wound Ostomy Cont. Nurs.*, **33**, S3 (2006).
3. L. G. Ovington, *Clin. Dermatol.*, **25**, 33 (2007).
4. C. K. Field and M. D. Kerstein, *Am. J. Surg.*, **167**, S2 (1994).
5. M. Santin, A. Motta, G. Freddi, and M. Cannas, *J. Biomed Mater. Res.*, **46**, 382 (1999).
6. G. H. Altman, F. Diaz, C. Jakuba, T. Calabro, R. L. Horan, J. Chen, H. Lu, J. Richmond, and D. L. Kaplan, *Biomaterials*, **24**, 401 (2003).
7. L. Meinel, S. Hofmann, V. Karageorgiou, C. Kirker-Head, J. McCool, G. Gronowicz, L. Zichner, R. Langer, G. Vunjak-Novakovic, and D. L. Kaplan, *Biomaterials*, **26**, 147 (2005).
8. S. Viju and G. Thilagavathi, *Fiber Polym.*, **13**, 782 (2012).
9. J. H. Kim, C. H. Park, Lee, O. J. Lee, J. M. Lee, J. W. Kim, Y. H. Park, and C. S. Ki, *J. Biomed. Mater. Res. Part A*, **100A**, 3287 (2012).
10. C. S. Ki, J. W. Kim, J. H. Hyun, K. H. Lee, M. Hattori, D. K. Rah, and Y. H. Park, *J. Appl. Polym. Sci.*, **106**, 3922 (2007).
11. W. H. Park, W. S. Ha, H. Ito, T. Miyamoto, H. Inagaki, and Y. Noishiki, *Fiber Polym.*, **2**, 58 (2001).
12. P. G. Chao, S. Yodmuang, X. Wang, L. Sun, D. L. Kaplan, and G. J. Vunjak-Novakovic, *Biomed. Mater. Res. Part B*, **95B**, 84 (2010).
13. X. Wang, T. Yucel, Q. Lu, X. Hu, and D. L. Kaplan, *Biomaterials*, **31**, 1025 (2010).
14. A. Sugihara, K. Sugiura, H. Morita, T. Ninagawa, K. Tubouchi, R. Tobe, M. Izumiya, T. Horio, N. G. Abraham and S. Ikehara, *Proc. Soc. Exp. Biol. Med.*, **225**, 58 (2000).
15. Y. H. Choi, M. G. Kim, D. H. Ahn, S. H. Hong, J. Lee, H. S. Kim, H. C. Kim, S. Y. Nam, and G. Yim, *J. Korean Surg. Soc.*, **79**, 421 (2010). (in Korean)
16. B. M. Min, L. Jeong, Y. S. Nam, J. M. Kim, J. Y. Kim, and W. H. Park, *Int. J. Biol. Macromol.*, **34**, 281 (2004).
17. S. E. Wharram, X. Zhang, D. L. Kaplan, and S. P. McCarthy, *Macromol. Biosci.*, **10**, 246 (2010).
18. A. Schneider, X. Y. Wang, D. L. Kaplan, J. A. Garlick, and C. Egles, *Acta Biomater.*, **5**, 2570 (2009).
19. P. Uttayarat, S. Jetawattana, P. Suwanmala, J. Eamsiri, T. Tangthong, and S. Pongpat, *Fiber Polym.*, **13**, 999 (2012).
20. A. Vasconcelos, A. C. Gomes, and A. Cavaco-Paulo, *Acta Biomater.*, **8**, 3049 (2012).
21. Z. Gu, H. Xie, C. Huang, L. Li, and X. Yu, *Int. J. Biol. Macromol.*, **58**, 121 (2013).
22. D. H. Roh, S. Y. Kang, J. Y. Kim, Y. B. Kwon, H. Y. Kweon, K. G. Lee, Y. H. Park, R. M. Baek, C. Y. Heo, J. Choe, and J. H. Lee, *J. Mater. Sci.-Mater. Med.*, **17**, 547 (2006).
23. S. Kanokpanont, S. Damrongsakkul, J. Ratanavaraporn, and P. Aramwit, *Int. J. Pharm.*, **436**, 141 (2012).
24. J. Rao, L. Ouyang, X. Jia, D. Quan, and Y. Xu, *Biomed. Eng.-Appl. Basis Commun.*, **23**, 1 (2011).
25. J. Draye, B. Delaey, A. V. Voorde, A. V. D. Bulcke, B. Bogdanov, and E. Schacht, *Biomaterials*, **19**, 9 (1998).
26. H. Jiang, D. Fang, B. S. Hsiao, B. Chu, and W. Chen, *Biomacromolecules*, **5**, 326 (2004).

27. F. Chen, Y. Zhao, H. Wu, Z. Deng, Q. Wang, W. Zhou, Q. Liu, G. Dong, K. Li, Z. Wu, and Y. Jin, *J. Control. Release*, **114**, 209 (2006).
28. A. Smelcerovic, Z. Knezevic-Jugovic, and Z. Petronijevic, *Curr. Pharm. Design*, **14**, 3168 (2008).
29. D. Chakravarthy and D. Smith, *J. Bioact. Compat. Polym.*, **10**, 313 (1995).
30. J. Draye, B. Delaey, A. V. Voorde, A. V. D. Bulcke, B. A. D. Reu, and E. Schacht, *Biomaterials*, **19**, 1677 (1998).
31. G. Sun, X. Zhang, Y. Shen, R. Sebastian, L. E. Dickinson, K. Fox-Talbot, M. Reinblatt, C. Steenbergen, J. W. Harmon, and S. Gerecht, *PNAS*, **108**, 20976 (2011).
32. H. K. Chenault, S. K. Bhatia, W. G. DiMaio, G. L. Vincent, W. Camacho, and A. Behrens, *Curr. Eye Res.*, **36**, 997 (2011).
33. V. A. Shkurupiy, M. A. Karpov, and N. G. Luzgina, *Bull Exp. Biol. Med.*, **153**, 647 (2012).
34. M. Rinaudo, *Polymers*, **2**, 505 (2010).
35. C. Mu, J. Guo, X. Li, W. Lin, and D. Li, *Food Hydrocolloids*, **27**, 22 (2012).
36. Y. Gong, G. Liu, W. Peng, X. Su, and J. Chen, *Carbohydr. Polym.*, **98**, 1360 (2013).
37. K. H. Lee, C. S. Ki, D. H. Baek, G. D. Kang, D. Ihm, and Y. H. Park, *Fiber. Polym.*, **6**, 181 (2005).
38. C. Perrino, S. Lee, S. W. Choi, A. Maruyama, and N. D. Spencer, *Langmuir*, **24**, 8850 (2008).
39. Y. Gotoh, M. Tsukada, N. Minoura, and Y. Imai, *Biomaterials*, **18**, 267 (1997).
40. T. Ouchi, T. Kontani, T. Saito, and Y. J. Ohya, *Biomater. Sci. Polym. Ed.*, **16**, 1035 (2005).